THE ASTROPHYSICAL JOURNAL, 526:L81–L84, 1999 December 1

SIMULTANEOUS X-RAY AND TeV OBSERVATIONS OF A RAPID FLARE FROM MARKARIAN 421

L. MARASCHI,[1] G. FOSSATI,[2] F. TAVECCHIO,[1] L. CHIAPPETTI,[3] A. CELOTTI,[4] G. GHISELLINI,[1] P. GRANDI,[5] E. PIAN,[6] G. TAGLIAFERRI,[1] A. TREVES,[7] A. C. BRESLIN,[8] J. H. BUCKLEY,[9] D. A. CARTER-LEWIS,[10] M. CATANESE,[10] M. F. CAWLEY,[11] D. J. FEGAN,[8] S. FEGAN,[12] J. FINLEY,[13] J. GAIDOS,[13] T. HALL,[13] A. M. HILLAS,[14] F. KRENNRICH,[12] R. W. LESSARD,[13] C. MASTERSON,[8] P. MORIARTY,[15] J. QUINN,[8] J. ROSE,[14] F. SAMUELSON,[10] T. C. WEEKES,[12] C. M. URRY,[16] AND T. TAKAHASHI[17]

Received 1999 July 16; accepted 1999 September 29; published 1999 October 27

ABSTRACT

Mrk 421 was observed for about 2 days with *BeppoSAX* in 1998 April as part of a worldwide multiwavelength campaign. A large, well-defined flare was observed in X-rays. The same flare was observed simultaneously at TeV energies by the Whipple Observatory gamma-ray telescope. These data provide (1) the first evidence that the X-ray and TeV intensities are well correlated on timescales of hours and (2) the first exactly simultaneous X-ray and TeV spectra. The results imply that the X-ray and TeV photons derive from the same region and from the same population of relativistic electrons. The physical parameters deduced from a homogeneous synchrotron self-Compton model for the spectral energy distribution yield electron cooling times close to the observed variability timescales.

Subject headings: BL Lacertae objects: individual (Markarian 421) — galaxies: active — galaxies: jets — gamma rays: observations — X-rays: galaxies

1. INTRODUCTION

It is now widely recognized that the strong and variable nonthermal emission of BL Lac objects originates in a relativistic jet pointed at a small angle to the line of sight. Radiation received from the jet is then amplified by relativistic effects, which accounts for its dominance and rapid variability (Blandford & Rees 1978).

Mrk 421 is the brightest BL Lac object at X-ray and UV wavelengths and the first extragalactic source discovered at TeV energies (Punch et al. 1992). Like most blazars (e.g., Sambruna, Maraschi, & Urry 1996; Ulrich, Maraschi, & Urry 1997; Fossati et al. 1998a), its spectral energy distribution shows two smooth broadband components. The first one extends from radio to X-rays with a peak in the soft to medium X-ray range; the second one includes the GeV to TeV emission with a peak presumed to be around 100 GeV. The emission up to X-rays is thought to be due to synchrotron radiation from high-energy electrons, while the spectral component peaking in the gamma-ray region is likely to derive from the same electrons via inverse Compton scattering of soft photons, thus accounting for the spectral "similarity" of the two components (Macomb et al. 1995; Ghisellini & Maraschi 1996; Mastichiadis & Kirk 1997; Tavecchio, Maraschi, & Ghisellini 1998). The fast variability observed in Mrk 421 at TeV energies (Gaidos et al. 1996) directly implies a minimum Doppler factor $\delta \sim 10$ (Celotti, Fabian, & Rees 1998).

If the above scenario is correct, a change in the density and/or spectrum of the high-energy electrons is expected to produce simultaneous variations at the frequencies emitted by the same electrons through the two processes. In particular, the two peaks present in the broadband spectral energy distribution should "correspond" to electrons of the same energy. Hence, a correlation between the X-ray and TeV emission is expected in Mrk 421. A measure of this correlation can provide strong constraints on theoretical models.

Previous observations at X-ray and TeV energies indeed yielded significant evidence of correlation on relatively long timescales but did not probe short timescales due to insufficient sampling (Macomb et al 1995; Catanese et al. 1997; Buckley et al. 1996). A new campaign was therefore organized in 1998 to obtain continuous coverage in X-rays for at least 1 week with *ASCA* complemented by other space and ground-based telescopes. Results from the overall campaign will be reported in T. Takahashi et al. (1999, in preparation; see also Takahashi, Madejski, & Kubo 1999). Here we discuss observations obtained between April 21 and 24 with the *BeppoSAX* satellite and the Whipple gamma-ray telescope, preceding the start of the *ASCA* observations. Preliminary results were presented in Maraschi et al. (1999a) and Catanese et al. (1999). The *BeppoSAX* observations in 1998 and 1997 will be fully presented by G. Fossati et al. (1999, in preparation, hereafter F99; see also Fossati et al. 1998b and Maraschi et al. 1999b). Relevant information about the observations is given in § 2, and

[1] Osservatorio Astronomico di Brera, via Brera 28, 20121 Milano, Italy.
[2] Center for Astrophysics and Space Science, University of California, San Diego, San Diego, CA 92093-0424.
[3] Instituto di Fisica Cosmica/CNR, via Bassini 15, 21133, Milano, Italy.
[4] Scuola Internazionale Superiore di Studi Avanzati/ISAS, via Beirut 2-4, 34014 Trieste, Italy.
[5] Istituto di Astrofisica Spaziale/CNR, via Fosso del Cavaliere, 00133 Roma, Italy.
[6] Istituto di Tecnologie e Studio delle Radiazioni Extraterrestri/CNR, via Gobetti 101, 40129 Bologna, Italy.
[7] Università del'Insubria, via Lucini 3, 22100 Como, Italy.
[8] Experimental Physics Department, University College, Belfield, Dublin 4, Ireland.
[9] Department of Physics, Washington University, St. Louis, MO 63130.
[10] Department of Physics and Astronomy, Iowa State University, Ames, IA 50011-3160.
[11] Physics Department, National University of Ireland, Maynooth, Ireland.
[12] Fred Lawrence Whipple Observatory, Harvard-Smithsonian Center for Astrophysics, Amado, AZ 85645.
[13] Department of Physics, Purdue University, West Lafayette, IN 47907.
[14] Physics Department, University of Leeds, Leeds, LS2 9JT, England, UK.
[15] School of Science, Galway-Mayo Institute of Technology, Galway, Ireland.
[16] Space Telescope Science Institute, 3700 San Martin Drive, Baltimore, MD 21218.
[17] Institute of Space and Astronautical Science, 3-1-1 Yoshinodai, Sagamihara, Kanagawa 229-8510, Japan.

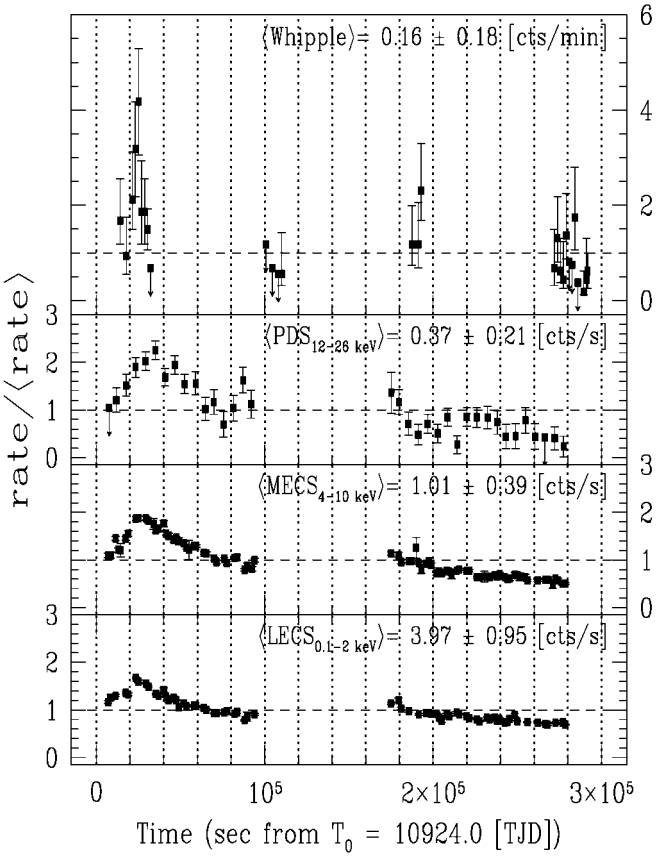

FIG. 1.—Light curves of Mrk 421 at TeV and X-ray energies. The first panel shows the Whipple data (>2 TeV), and the second, third, and fourth panels refer to *BeppoSAX* data with energy ranges as specified. All the count rates were normalized to their respective averages (given in each panel) over the observations shown.

the results are presented in § 3 and discussed in § 4. Section 5 summarizes the conclusions.

2. OBSERVATIONS

2.1. *BeppoSAX Observations*

The scientific payload carried by *BeppoSAX* is described in Boella et al. (1997a). The data of interest here derive from three co-aligned instruments, the Low-Energy Concentrator Spectrometer (LECS; 0.1–10 keV; Parmar et al. 1997), the Medium-Energy Concentrator Spectrometer (MECS; 2–10 keV; Boella et al. 1997b), and the Phoswich Detector System (PDS; 12–300 keV; Frontera et al. 1997). For a short account of information relevant here, see Chiappetti et al. (1999).

Two observations were obtained with *BeppoSAX*, covering the time intervals from 1998 April 21 (01:59 UT) to April 22 (03:13 UT) and from 1998 April 23 (00:28 UT) to April 24 (06:37 UT). The net exposure times in the MECS and LECS, respectively, were 34,000 and 23,600 s for the first observation and 40,000 and 27,200 s for the second one. The data reduction for the PDS was done using the XAS software (Chiappetti & Dal Fiume 1997), while for the LECS and MECS, linearized cleaned event files generated at the *BeppoSAX* Science Data Center were used and reduced with the standard software packages FTOOLS 4.2 and XSPEC 10. No appreciable difference was found extracting the MECS data with the XAS software. For a detailed description of the analysis procedure, we refer the reader to F99.

2.2. *Whipple Observations*

The very high energy gamma-ray observations were made with the Whipple Observatory 10 m telescope (Cawley et al. 1990). At the time of these observations, the telescope camera consisted of 331 circular-face photomultiplier tubes (PMTs) with a combined field of view of 4°.8. The event trigger condition was that any two of the 331 PMTs register a signal over 40 photoelectrons within a coincidence overlap time of 8 ns. Also, light cones were not in place and this, as well as reduced reflectivity of the mirrors, resulted in a somewhat higher energy threshold than usual for the telescope; hence, for these observations the energy threshold was ~500 GeV.

Events were parameterized with a standard moment analysis, and candidate gamma rays were selected using a variation of the Supercuts analysis (Reynolds et al. 1993) appropriate for the large camera field of view and for maintaining a constant energy threshold as a function of observation elevation (see Catanese et al. 1999 and discussion below).

Observations were taken on the nights of 1998 April 21, 22, 23, and 24. To permit several hours of observations within each night, data were taken over a large range of zenith angles (~7°–60°). The collection area and energy threshold increase with zenith angle and the gamma-ray selection is a function of zenith angle, yielding spurious changes in the observed gamma-ray rates. To obtain the intrinsic light curve, it was necessary to determine special, elevation-dependent, software cuts. Because contemporaneous observations of the Crab Nebula were not available with sufficient statistics over all the zenith angles, the analysis presented here relies entirely on Monte Carlo shower simulations.

Simulated gamma-ray–induced showers at zenith angles of 20°, 40°, 45°, and 55° were generated with ISUSIM (Mohanty et al. 1998) to determine the size cut required at each zenith angle to obtain a common energy threshold of 2 TeV and to estimate the collection areas at these zenith angles for the 2 TeV energy threshold. After reduction to the common energy threshold of 2 TeV, the measured rates were renormalized using effective area ratios of 1.0 : 1.5 : 2.6 : 4.7 for the four zenith angle ranges, respectively.

3. RESULTS

3.1. *Light Curves*

A large well-defined flare was seen during the first day of observation with *BeppoSAX*. The light curves in three energy bands (0.1–2, 4–10, and 12–26 keV) normalized to their respective means are shown in Figure 1. The energy ranges were chosen so as to represent well-separated "effective" energies with reasonable statistics. Given the source average spectrum and the instrumental response of the LECS, MECS, and PDS, these energies can be estimated as $\simeq$1, $\simeq$5, and $\simeq$15 keV for the three energy bands, respectively. The flare amplitude increases slightly with energy: the flux ratios at two fixed epochs (3×10^4 and 7×10^4 s after observation start) are 1.5, 1.6, and 1.9 for the three energy bands, respectively. Fitting the decays of the three light curves with simple exponentials in the same time interval yields e-folding timescales τ_e of 10.7 (10–11.5) $\times 10^4$, 7.1 (6.6–7.7) $\times 10^4$, and 5.3 (3.7–8.7) $\times 10^4$ s, respectively, where the given intervals correspond to

90% confidence for one parameter. We note that the choice of fitting with a simple exponential is somewhat arbitrary. More detailed timing analysis is in progress (F99).

The event rates from the Whipple Cerenkov Telescope above the 2 TeV threshold are also shown in Figure 1, normalized to the average of the four nights. A clear peak is present with amplitude $\simeq$4 times the mean flux level and a halving time of about 1 hr. Here the error is large due to the low statistics. An exponential fit to the TeV light curve gives a decay time $\tau = 5 \times 10^3$ s [(3–8) $\times 10^3$ s, at 1 σ], which is shorter than that found at X-ray energies.

Assuming that the peak of the 2 TeV light curve falls within the three highest points defines an uncertainty interval of 1.5 hr. The peaks of the 0.1–2 and 4–10 keV light curves fall within this interval, while the 12–26 keV light curve seems to peak later, although the significance of this effect needs to be assessed. We can therefore conclude that the TeV flare and the medium-energy X-ray flare are simultaneous to within ± 1.5 hr. The presence of possible (small) leads/lags between light curves at different energies (first detected by Takahashi et al. 1996) is under study.

3.2. *Spectra*

Integrating the X-ray and TeV events for the duration of the TeV observations during the first night, we can obtain exactly simultaneous X-ray and TeV spectra.

Acceptable fits to the X-ray data require curved models: at least three power laws are required to model the combined LECS and MECS data (Fossati et al. 1998b; Maraschi et al. 1999b; F99). These spectral properties are common to PKS 2155−304 and Mrk 501 (Chiappetti et al. 1999; Pian et al. 1999). For consistency with the theoretical model used below, we adopted a continuously curved spectral law with two "asymptotic" slope values, given by $F(E) = KE^{-\alpha_1}[1 + (E/E_{\rm break})]^{\alpha_1-\alpha_2}$. Absorption was fixed at the Galactic value $N_{\rm H} = 1.61 \times 10^{20}$ cm^{-2} (Lockman & Savage 1995). The derived values of the fitted parameters are $\alpha_1 = 0.52$ (0.24–0.7), $\alpha_2 = 2.0$ (1.9–2.2), and $E_{\rm break} = 2.0$ (1.4–2.9) keV. The spectrum deconvolved with the above model is shown in Figure 2.

The spectral energy distribution of the TeV photons has been calculated excluding data at large zenith angles. The standard analysis as described by Mohanty et al. (1998) has been applied. Individual data points are shown in Figure 2. The resulting spectrum is well represented by a simple power law: $F(E) = 3.17 \times 10^{-7}\,(E/1\ {\rm TeV})^{-2.53\pm0.18}$ photons m^{-2} s^{-1} TeV^{-1}, consistent with other flare spectra (Krennrich et al. 1999).

Also shown in Figure 2 are two gamma-ray spectra measured by EGRET (Macomb et al. 1995; Sreekumar et al. 1996). UV data represent historical maximum, minimum, and average fluxes recorded by *IUE* in the period 1979–1990 (see Edelson 1992; Pian & Treves 1993). Optical data are from the 1994–1997 optical campaign reported by Tosti et al. (1998) excluding the large 1997 outburst.

4. DISCUSSION

The good temporal correlation between the TeV and X-ray flares on short timescales, demonstrated by these data for the first time, supports models in which the high-energy radiation arises from the same population of electrons that produce the X-ray flare via synchrotron radiation. The most likely mechanism is inverse Compton scattering of soft photons. Since the LECS and MECS peaks coincide with the TeV peak within

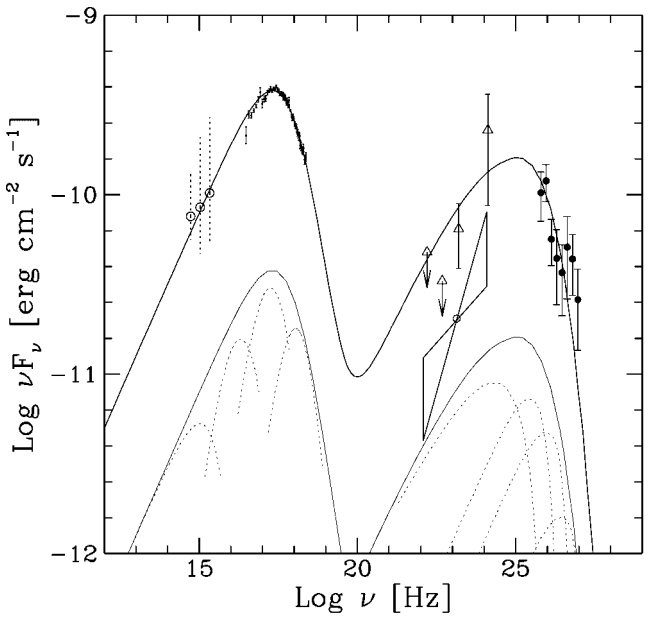

FIG. 2.—SED of Mrk 421. The simultaneous spectral data in the X-ray and TeV ranges are shown as dots. Historical EGRET data (*triangles and open circle*) are taken from Macomb et al. (1995) and Sreekumar et al. (1996). UV fluxes are the averages, and the bars represent maximum and minimum fluxes recorded by *IUE* in the period 1979–1990. Optical data are from the 1994–1997 optical campaign excluding the large 1997 outburst. The solid line is the spectrum calculated with the SSC model as described in the text. We also show the contribution to the total spectrum (*thin solid line*, downshifted by one decade) of electrons with different energies (*dotted lines*). From the left the curves show the emission from electrons with Lorentz gamma factor in the range 10–3 $\times$ 10^4, 3 $\times$ 10^4–10^5, 10^5–3 $\times$ 10^5 and 3 $\times$ 10^5–10^6.

± 1.5 hr, the spatial separation of the X-ray– and TeV–emitting regions must be less than $(2 \times 10^{14})\,\delta$ cm ($\delta = [\Gamma(1 - \beta\cos\theta)]^{-1}$, where Γ is the bulk Lorentz factor $\beta = v/c$ and θ is the angle between the line of sight and the direction of motion).

The spectral energy distribution (SED) obtained by combining simultaneous X-ray and TeV data can be used to accurately estimate the physical parameters of the emitting region. In Figure 2, we show the spectrum from a homogeneous synchrotron self-Compton (SSC) model computed with the full Klein-Nishina cross section (Jones 1968) and assuming for the electron energy distribution a curved shape with a smooth transition between two asymptotic slopes, $N(\gamma) = K\gamma^{-n_1}[1 + (\gamma/\gamma_{\rm break})]^{n_1-n_2}$, consistent with that used to deconvolve the X-ray data. The parameters which best approximate the observed SED are $B = 0.06$ G, $R = 10^{16}$ cm, $\delta = 20$, $n_1 = 2.2$, $n_2 = 5.3$, $K = 4 \times 10^4$, and $\gamma_{\rm break} = 3 \times 10^5$.

The homogeneous model is tightly constrained by the data. In fact, in order to account for the relatively flat TeV spectrum, the peak of the inverse Compton component must occur very close to the TeV band. Since the inverse Compton peak is affected by the Klein-Nishina limit, this forces a rather low value of the magnetic field (see Tavecchio, Maraschi, & Ghisellini 1998). Comparing the magnetic energy density $u_B = 1.4 \times 10^{-4}$ with the particle energy density $u_e = 0.16\gamma_{\rm min}^{-0.2}$ (where $\gamma_{\rm min}$ is the lower limit of the electron energy spectrum), one finds that the magnetic field is largely below equipartition. The energy flux in the jet (see, e.g., Bicknell & Dopita 1997) is $F_E = 8 \times 10^{44}\gamma_{\rm min}^{-0.2}(1 + 0.95\chi)$ ergs s^{-1}, where, for $n_e = n_p$, $\chi = 230\gamma_{\rm min}^{-1}$. Therefore, depending on χ and $\gamma_{\rm min}$, it ranges from

10^{44} to 10^{47} ergs s^{-1}, which is similar to other BL Lac objects (e.g., Celotti, Padovani, & Ghisellini 1997).

In the lower part of Figure 2 we show the separate contributions of electrons in different energy ranges to the synchrotron and inverse Compton radiation, respectively. The four subcomponents refer to electrons with Lorentz factors $\gamma < 3 \times 10^4$, $3 \times 10^4 < \gamma < 10^5$, $10^5 < \gamma < 3 \times 10^5$, and $3 \times 10^5 < \gamma < 10^6$, belonging to the assumed overall spectrum. The inverse Compton emission is computed in each case using all the synchrotron photons. Electrons in the third energy range contribute mostly near the peak of the synchrotron emission. The peak of the inverse Compton emission is due to electrons in the first and second energy ranges, while the contribution from the third is depressed by the Klein Nishina limit. Above 2 TeV, which is the energy threshold for the light curve shown in Figure 1, the third and fourth components—that is, precisely those that contribute in the X-ray band—are the largest contributors.

It is interesting to compute the decay of the electron population determined from the spectral fit under the simple hypothesis of an impulsive injection followed by radiative cooling. This is somewhat different from estimating the radiative lifetime of electrons of a given energy and involves also the time dependence of the *number* of particles at a given energy, which depends on the particle spectrum.

We derived flux halving times of 1.1×10^4 s at 1 keV and of 5×10^3 s at 2 TeV. These should be compared with observed halving times ($\tau_{1/2} = 0.7\tau_e$) of 7.4×10^4 and 3.4×10^3 s, respectively. Given the simplicity of the model and the fact that its parameters have been *independently* derived from the *spectral* fit, we consider this result remarkable, even if the observed time at 1 keV is larger than computed. This indicates that radiative cooling can play an important role in the flare decay but cannot be the only process involved. Moreover, the timescales computed with this simple hypothesis are energy dependent, decreasing roughly as the square root of the energy in the X-ray band and linearly with energy in the TeV band. While we cannot at present split the TeV light curve in different energy bands, the X-ray light curves show an energy dependence that is weaker than predicted.

Finite acceleration and injection times plus light-travel time effects need to be included in more realistic models in addition to radiative losses. It is not obvious, however, how these could affect the X-ray and TeV emission differently unless the hypothesis of a homogeneous source is also abandoned. Work along these lines has been done; more is in progress (Kirk, Rieger, & Mastichiadis 1998; Chiaberge & Ghisellini 1999; Dermer 1998; Kataoka et al. 1999; F99), but it involves computations beyond the scope of the present Letter.

5. CONCLUSIONS

A strong flare in Mrk 421 was observed to occur simultaneously, to within ± 1 hr, at X-ray and TeV wavelengths, and an exactly simultaneous X-ray–to–TeV energy distribution (averaged over the flare) could be obtained. The simultaneity of the flare peaks implies that the particles radiating in the two bands are spatially close, and the observed SED implies that they belong to the same energy range. The parameters of the emission region are tightly constrained, and the resulting cooling times for the electrons radiating in the X-ray and TeV bands are close to the observed timescales. This coincidence suggests that the cooling process plays a role in the flare evolution, although more complex models are needed to fully account for the multiwavelength time behavior.

Multiwavelength observations of this and similar sources, including the UV band in which cooling times are necessarily much longer, will be critical to assess the roles of the different processes and to disentangle possibly multiple emission regions. *X-Ray Multimirror Mission*, with its broadband capabilities, together with the next generation of atmospheric Cerenkov telescopes, which yields detailed light curves of TeV flares in different energy bands, seem ideally suited to perform such programs.

We thank G. Bicknell for helpful comments. This work was supported in part by ASI grant ARS-98-91 and by the European Commission under contract number ERBFMRX-CT98-0195. A. C. acknowledges financial support from the Italian MURST and the National Science Foundation (grant PHY 94-07194).

REFERENCES

Bicknell, G. V., & Dopita, M. A. 1997, in Relativistic Jets in AGNs, ed. M. Ostrowski (Kraków: Uniwersytet Jagiellonski, Obs. Astron.), 1
Blandford, R. D., & Rees, M. J. 1978, in BL Lac Objects, ed. A. M. Wolfe (Pittsburgh: Univ. Pittsburgh Press), 328
Boella, G., et al. 1997a, A&AS, 122, 299
———. 1997b, A&AS, 122, 327
Buckley, J. H., et al. 1996, ApJ, 472, L9
Catanese, M., et al. 1997, ApJ, 487, L143
———. 1999, Proc. 26th Int. Cosmic-Ray Conf. (Salt Lake City), 3, 305
Cawley, M. F., et al. 1990, Exp. Astron., 1, 173
Celotti, A., Fabian, A. C., & Rees, M. J. 1998, MNRAS, 293, 239
Celotti, A., Padovani, P., & Ghisellini, G. 1997, MNRAS, 286, 415
Chiaberge, M., & Ghisellini, G. 1999, MNRAS, 306, 551
Chiappetti, L., & Dal Fiume, D. 1997, in Proc. Fifth Workshop on Data Analysis in Astronomy, ed. V. Di Gesú (Singapore: World Scientific), 101
Chiappetti, L., et al. 1999, ApJ, 521, 552
Dermer, C. D. 1998, ApJ, 501, L157
Edelson, R. A. 1992, ApJS, 83, 1
Fossati, G., et al. 1998a, MNRAS, 299, 433
———. 1998b, Nucl. Phys. B Proc. Suppl., 69, 423
Frontera, F., et al. 1997, A&AS, 122, 357
Gaidos, J. A., et al. 1996, Nature, 383, 319
Ghisellini, G., & Maraschi, L. 1996, in ASP Conf. Ser. 110, Blazar Continuum Variability, ed. H. R. Miller, J. R. Webb, & J. C. Noble (San Francisco: ASP), 436
Jones, F. C. 1968, Phys. Rev., 167, 1159
Kataoka, J., et al. 1999, ApJ, in press
Kirk, J. G., Rieger, F. M., & Mastichiadis, A. 1998, A&A, 333, 452
Krennrich, F., et al. 1999, ApJ, 511, 149
Lockman, F. J., & Savage, B. D. 1995, ApJS, 97, 1
Macomb, D. J., et al. 1995, ApJ, 449, L99 (erratum 459, L111 [1996])
Maraschi L., et al. 1999a, Astropart. Phys., 11, 189
———. 1999b, Proc. 32nd COSPAR Meeting (Amsterdam: Elsevier), in press (astro-ph/9902059)
Mastichiadis, A., & Kirk, J. G. 1997, A&A, 320, 19
Mohanty, G., et al. 1998, Astropart. Phys., 9, 15
Parmar, A. N., et al. 1997, A&AS, 122, 309
Pian, E., et al. 1999, in ASP Conf. Ser. 159, BL Lac Phenomenon, ed. L. Takalo (San Francisco: ASP), 180
Pian, E., & Treves, A. 1993, ApJ, 416, 130
Punch, M., et al. 1992, Nature, 358, 477
Reynolds, P. T., et al. 1993, ApJ, 404, 206
Sambruna, R. M., Maraschi, L., & Urry, C. M. 1996, ApJ, 463, 444
Sreekumar, P., et al. 1996, ApJ, 464, 628
Takahashi, T., Madejski, G., & Kubo, H. 1999, Astropart. Phys., 11, 177
Takahashi, T., et al. 1996, ApJ, 470, L89
Tavecchio, F., Maraschi, L., & Ghisellini, G. 1998, ApJ, 509, 608
Tosti, G., et al. 1998, A&A, 339, 41
Ulrich, M. H., Maraschi, L., & Urry, C. M. 1997, ARA&A, 35, 445